Modelling in-plane dynamic response of a fastening system for horizontal concrete facade panels in RC precast buildings

Gabrijela Starešinič[a,*], Blaž Zoubek[b], Matija Gams[a], Tatjana Isaković[a], Matej Fischinger[a]

[a] Faculty of Civil and Geodetic Engineering, University of Ljubljana, Jamova 2, 1000 Ljubljana, Slovenia
[b] Schimetta Consult Ziviltechniker Ges.m.b.H., Landwiedstraße 23, 4020 Linz, Austria

ABSTRACT

The paper presents experimental and analytical studies of the dynamic in-plane response of typical fastening systems for horizontal cladding panels in RC precast industrial buildings in Central Europe. The system consists of two main parts: a pair of top bolted connections, which provide the horizontal stability of the panel, and a pair of bottom cantilever connections, which support the weight of the panel. A typical response mechanism of the fastening system consists of three distinct stages: sliding with limited friction, contact with the panel causing an increase in the connection stiffness, and failure. It has been found that the capacity of the complete system is limited by the displacement capacity of the top connections, which are the most critical components. Therefore, it is better to express the capacity of the entire system in terms of displacements.

Appropriate numerical models for the complete fastening system have been proposed and validated by the results of the presented experiments. The top and bottom connections were analysed separately and showed physically different response behaviours. The typical Coulomb friction model was used to describe the friction in the top connection, whereas the viscous friction model better simulated variable friction in the bottom connection. The contacts that occur when the gap for sliding of panels closes were simulated by an abrupt increase of the stiffness of the connection.

1. Introduction

Precast industrial buildings house a large share of the European industrial activity. Because of their rapid construction, open space and low cost, they are becoming a more and more popular structural system all over Europe. As observed during the past earthquakes in Northern Italy, if these buildings had not been adequately designed, their damage or collapse could have caused considerable direct and indirect economic losses due to production disruption [1–3].

To avoid such consequences, comprehensive systematic studies of RC precast buildings were performed within several EU research projects combining the efforts of industry and different academic institutions. The last joint EU project SAFECLADDING [4] was devoted to the connections of the façade cladding panels to the main structural system of industrial buildings with the main aim of improving the related design practice.

Before SAFECLADDING and some parallel studies [5–7] were conducted, the knowledge about the seismic response of cladding panels was very poor, and even the basic mechanisms of seismic response were not known. The design practice was also inadequate. It only considered

the out-of-plane response [8] instead of the more critical horizontal direction parallel to the plane of the panels [9,10]. This has also been confirmed in the recent earthquakes in Northern Italy, where the failure of the fastening system was one of the main reasons for the collapse of cladding panels [9]. Examples of the collapses in the Emilia Romagna earthquake are shown in Fig. 1.

The comprehensive experimental [11,12] and analytical studies performed within the aforementioned European project considerably improved the knowledge about the seismic response of the cladding panels' fastening systems. Three different basic concepts were assessed and considered within the studies: the *integrated* solution where the connections provide full integration of the cladding panels into the main structural system [13], the *dissipative* solution where the fastening system of the cladding panels is used as the important source of energy dissipation [12,14], and the *isostatic* solution where the fastenings allow the relative displacements between the panels and the main structural system, keeping the panels as non-structural elements.

The part of the research, performed at the University of Ljubljana - UL [10], was devoted to the fastenings systems of vertical [15] and horizontal cladding panels, which are widely used in the existing

* Corresponding author.
  E-mail address: gabrijela.staresinic@fgg.uni-lj.si (G. Starešinič).
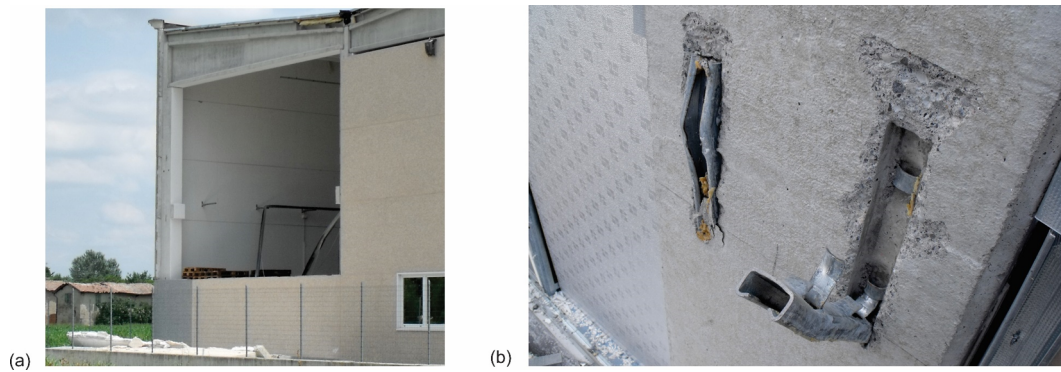
Fig. 1. (a) Failure of the cladding panels and (b) the damaged cladding connections during the earthquake in Emilia Romagna.

practice in Central Europe. The SAFECLADDING project significantly raised the awareness of many problems with the existing design and construction practice for cladding systems and has resulted in new design guidelines for precast structures with cladding panels [16] and for wall panel connections [17].

Similar research campaigns, however not included in the SAFECLADDING project, were performed in parallel with the mentioned project. The in-plane and the out-of-plane seismic response of the connections, which are used to fasten the horizontal cladding panels, was experimentally and analytically studied by Belleri et al. [5,6]. The isostatic types of the connections for vertical and horizontal panels were extensively investigated by Del Monte et al. [7], whom successfully modified the cladding connections to improve their displacement capacity.

Although many important observations about the seismic response of cladding panels, typical for Central Europe, have been obtained at the UL within the SAFECLADDING project, this research could not completely reveal and explain all the aspects of this complex response. It was not possible to fully determine the role of panels' fastenings and their realistic boundary conditions without a more complex study of the whole system response. To get the answers to these questions, research has been continued within the research project ″Seismic resilience and strengthening of precast industrial buildings with concrete claddings″, funded by the Slovenian Research Agency. One of the main phases of this project is devoted to the full-scale shake table experiments of RC building with cladding panels. To be able to set-up these highly complex tests, studies of the single components, performed within SAFECLADDING, were complemented by additional cyclic and dynamic tests, to obtain as much data as possible about their basic seismic response mechanisms and their capacity. The experimental studies were followed by analytical studies which dealt with different possibilities for the numerical modelling of the investigated fastening systems. In this paper, the part of the research campaign devoted to dynamic tests of connections for the horizontal panels is presented. Test results were used to develop a new numerical model and calibrate the parameters.

The studied fastening system consists of two main parts: (1) a pair of top bolted connections, which provide the stability of the panel, subjected to the horizontal excitations, and (2) a pair of bottom cantilever connections, which support the weight of the panel. This fastening system is the so-called seated isostatic connection system, which is supposed to provide horizontal relative displacements between the panel and the main structure of the building at the upper side of the panels. To augment mostly monotonic and cyclic tests of single connections [5,7,13–15], the dynamic tests of the fastening system are presented in this paper. The response of the cladding connections was investigated in the in-plane direction, which has been recognised as critical in a survey of precast structures after the L'Aquila earthquake [9]. It should be noted, that in some papers, which deal with structures without roof diaphragm and develop significant torsion, higher load

demand is reported in the out–of–plane direction [6,18]. Such structures are not considered in this paper.

The investigated fastening system and test setup are presented in Section 2 and Section 3, respectively. In Section 4, the test results and observations are analysed. Typical response mechanisms of the components and the complete fastening system are presented, and the main response parameters are discussed. In Section 5, the numerical model for the simulation of the hysteretic response of the investigated fastening system is proposed and validated by the results of the performed experiments.

2. Description of the tested connections

The fastening system investigated within the presented research campaign is one of the most common systems used in Central Europe to attach horizontal cladding panels to the columns of RC precast structures. It consists of a bolted connection attaching the top part of the panel and a cantilever connection attaching the bottom part of the panel to the columns of the building (Fig. 2).

The top connection (Fig. 3) is intended to provide the stability of the panel and the relative displacements between the panel and the columns when the structure is subjected to horizontal excitations. It consists of a vertical steel channel built into the column, and a special box-shaped steel element, which is cast in the panel as presented in Fig. 3. These two elements are connected using a special hammer-head bolt, which is set inside the channel (cast in the column) and on the other side firmly secured to the steel box element (cast in the panel). Bolts HS 40/22M16 are typically used to attach panels to the columns.

The bottom component of the fastening system is the cantilever connection (Fig. 4), which is placed at the bottom corners of the panel. The primary role of the bottom connection is to support the weight of the panel. It consists of a special steel box, which is inserted in the column before casting, and a steel plate, which is cast into the panel. During the mounting of the panels, the cantilever steel bracket is placed in the steel box in the column and anchored to it using a skewed bolt. The panel simply lays on this steel cantilever element. As can be seen in Fig. 4, the panel is actually supported by the steel studs fastened to the top of the cantilever brackets, which are used to regulate the level of the panel to account for tolerances. Finally, the panel is secured at the top with the hammer-head bolts.

3. Description of the experiments

3.1. Description of the tested specimens and test setup

Two sets of experiments were performed:

(1) tests of the top connections, and
(2) tests of the complete fastening system consisting of top and bottom connections.
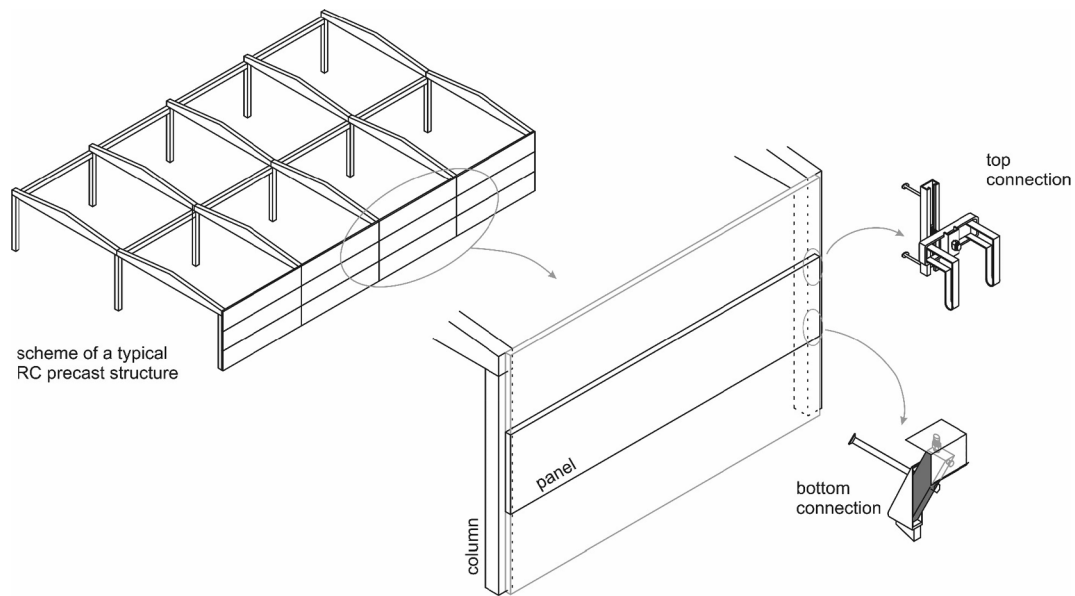
Fig. 2. Scheme of a typical RC precast structure with horizontal panels.

The general setup of the experiments is illustrated in Figs. 5 and 6. The inverted T-shaped beam was fixed to the laboratory floor. The panel was placed in parallel to the beam and connected to it by using the fastening system. In the tests of the top connections (Fig. 5a, b, c), the bottom of the panel was mounted on specially designed rollers, which allowed for the friction-free movement of the panel parallel to the foundation beam. In the tests of the complete fastening system (Fig. 5d, e, f), the bottom of the panel was supported by the cantilevers. An actuator was connected to the panel, as illustrated in Fig. 5 (c, f).

To perform as many experiments as possible, the foundation block was designed so that it could be used for two sets of tests on each side. The top connections were tested in pairs. The inner two top connections were used for one set of tests and the outer two connections for the other set of tests (Fig. 5b). The distance between the connections was 45 cm in the case of the inner two connections, and 135 cm in the case of the outer two. Although this configuration differs from the real application of the system where connections are at the end of the several meters long panels, the simplification is justifiable because the panels act as translationally moving rigid bodies in both cases. The same approach was used to test the complete fastening system, consisting of two top and two bottom connections (Fig. 5e).

3.2. Summary of the performed experiments and loading protocol

In total, six dynamic tests were performed, as summarized in Table 1. Four dynamic tests were performed on the top connections and two dynamic tests on the complete fastening system.

The loading protocol for the dynamic tests was defined based on the estimated displacements and velocities in the connections of an actual building and taking into account the capacity of the hydraulic system. An actuator with a static capacity of 250 kN (with a $\pm$ 200 mm stroke) was used. However, when performing dynamic tests, the capacity of the actuator is managed by the capacity of the hydraulic system, and the maximum force capacity is co-dependent on the applied velocities.

In order to estimate the range of displacements and velocities, the response-history analysis of a structure, planned to be tested on the shaking table, was considered. In the analysis, the generated accelerogram, corresponding to the acceleration spectrum matching the Eurocode acceleration design spectrum for soil type B, was used (see [19] for more details). The applied displacement response history was defined, taking into account these analytical studies as well as the capacity of the actuator used in the tests.

Each test consisted of several runs. The displacement amplitude
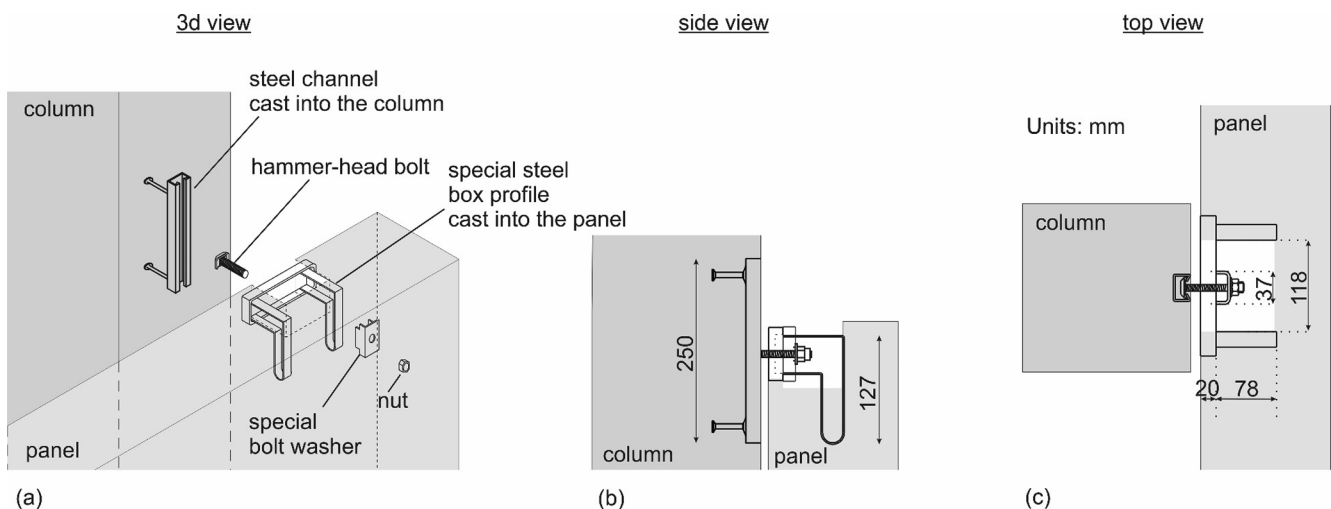
Fig. 3. The assembly of the top connection under consideration: (a) 3d view, (b) side view and (c) top view.
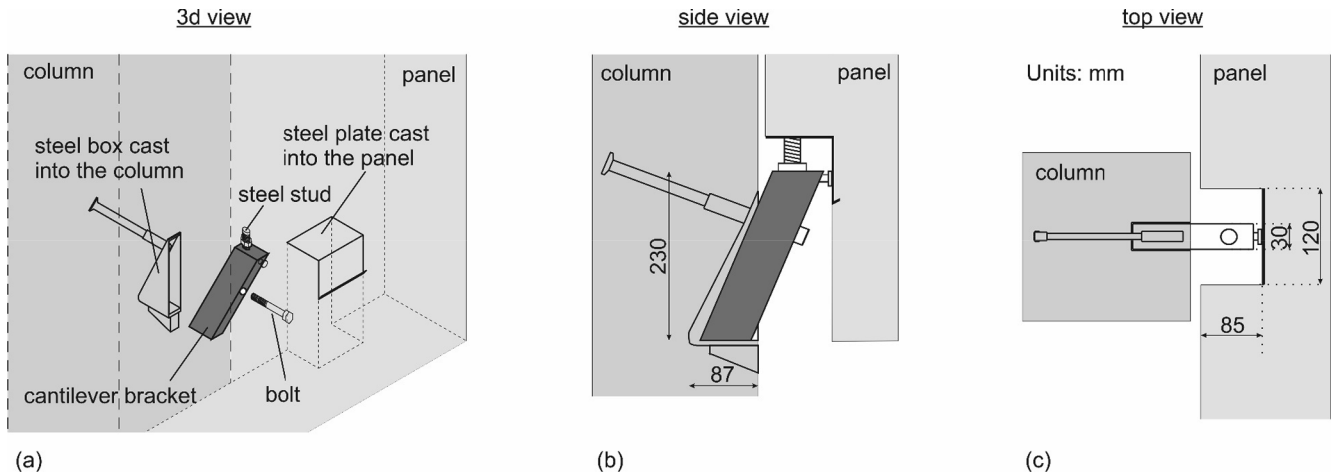
Fig. 4. The assembly of the bottom connection under consideration: (a) 3d view, (b) side view and (c) top view.

TESTS OF THE TOP CONNECTIONS
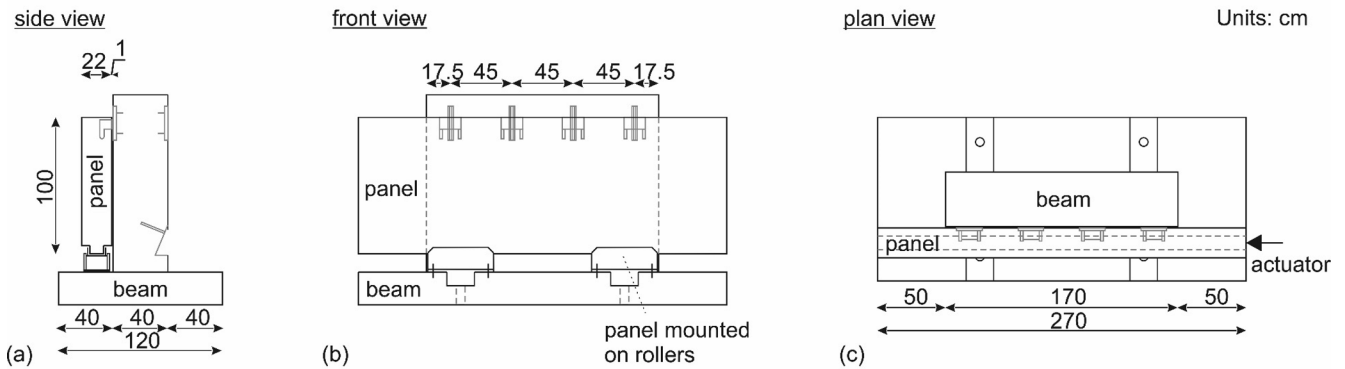
TESTS OF THE COMPLETE FASTENING SYSTEM
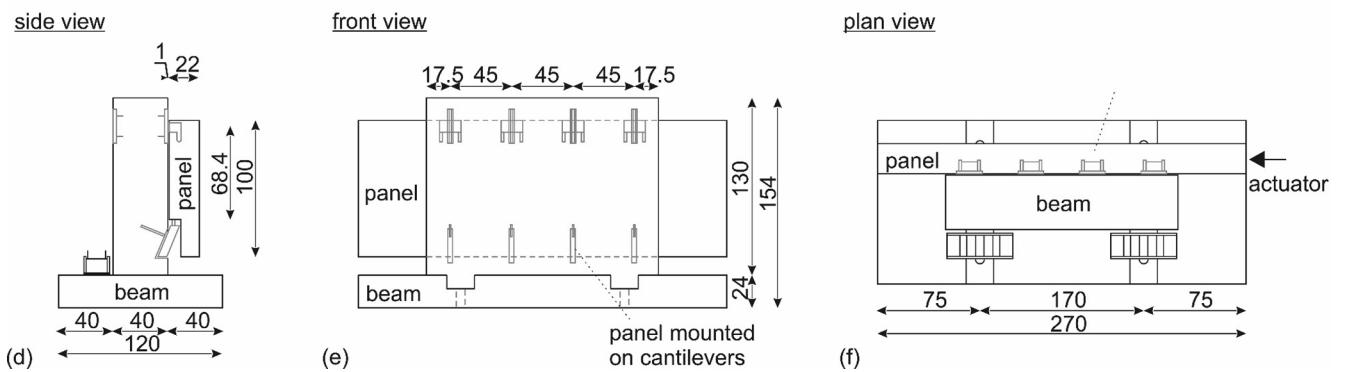
Fig. 5. The general arrangement of the experimental setup: (a) side view of the specimen with the top connections, (b) front view of the specimen with the top connections (c) plan view of the specimen with the top connections, (d) side view of the specimen with the complete fastening system, (e) front view of the specimen with the complete fastening system, and (f) plan view of the specimen with the complete fastening system.

(and consequently also the velocities) gradually increased up to the failure of the connections, or the capacity of the actuator. The applied dynamic load (displacements and velocities) that corresponds to the scale factor 1.0 (see also Table 1) is shown in Fig. 7. When the top connections were tested, the bolts were retightened to 65 Nm before each run. In tests of the complete fastening system, the bolts were tightened to 65 Nm only before the first run.

4. Results and observations of the experiments

The test results are presented in the form of force–displacement hysteretic responses. Since the strong and stiff foundation beam was fixed to the laboratory floor and the displacements were imposed only to the panel, processing of the results was straightforward. The sum of forces in the tested connections is the same as the recorded forces in the
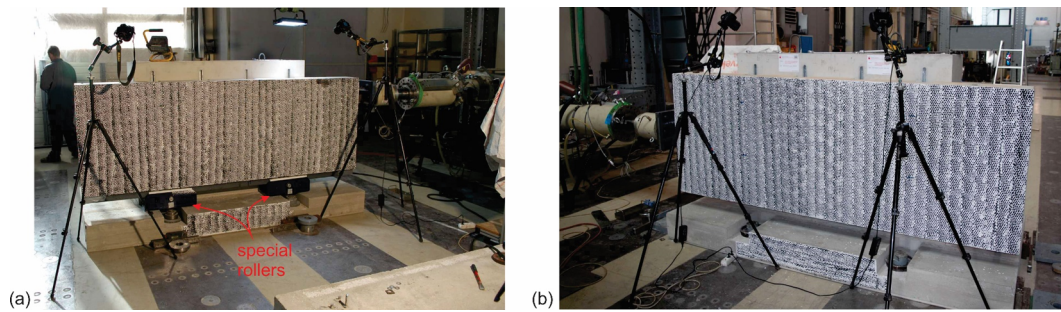
Fig. 6. The experimental setup during testing (a) the top connections and (b) the complete fastening system.

Table 1
Summary of the dynamic experiments.

Test	Type of the connections	Scale factor for test run	Max displacement [cm]	Max velocity [m/s]
T1	Top connections	0.5 / 1.0 / 1.5 / 2.0 / 2.5	8.2	0.10
T2	Top connections	1.0 / 2.0 / 3.0	11.0	0.13
T3	Top connections	1.0 / 2.0 / 3.0	11.0	0.13
T4	Top connections	1.0 / 2.0 / 3.0	11.0	0.13
C1	Complete fastening system	1.0 / 1.1 / 1.2 / 1.5 / 1.6	5.9	0.07
C2	Complete fastening system	1.0 / 1.2 / 1.4 / 1.5 / 1.6	5.9	0.07

actuator, and the imposed displacements correspond to the relative displacements of each connection. This was confirmed with the optical deformation measuring system GOM Aramis 5M [20] which was also used. The main reason for the use of the optical system was to control the movements of the panel in the vertical direction, which were found to be negligibly small.

4.1. Response mechanism of the top bolted connections

Typical force–displacement hysteretic responses of the top connections are presented in Fig. 8. On each plot, the results of all the runs performed within the addressed test are shown. The response consists of three main stages, as presented in Fig. 9 and marked with dots in Fig. 8:

(1) In the first phase (between dots 1 and 2) the bolt slides along the steel box profile cast in the panel (see Figs. 8 and 9). At this stage, a limited friction force of about 10–16 kN (corresponding to the pair of connections) is activated. Its amount depends on the tightening moment applied to the bolt and the coefficient of friction between the special steel washer and the steel box profile cast in the panel (see Fig. 9).

(2) The second stage (between dots 2 and 3) starts when the bolt washer reaches the edge of the steel box (see Fig. 9b), corresponding to the slip of the bolt $d_{slip} = 3\text{–}4$ cm. At this stage, the bolt
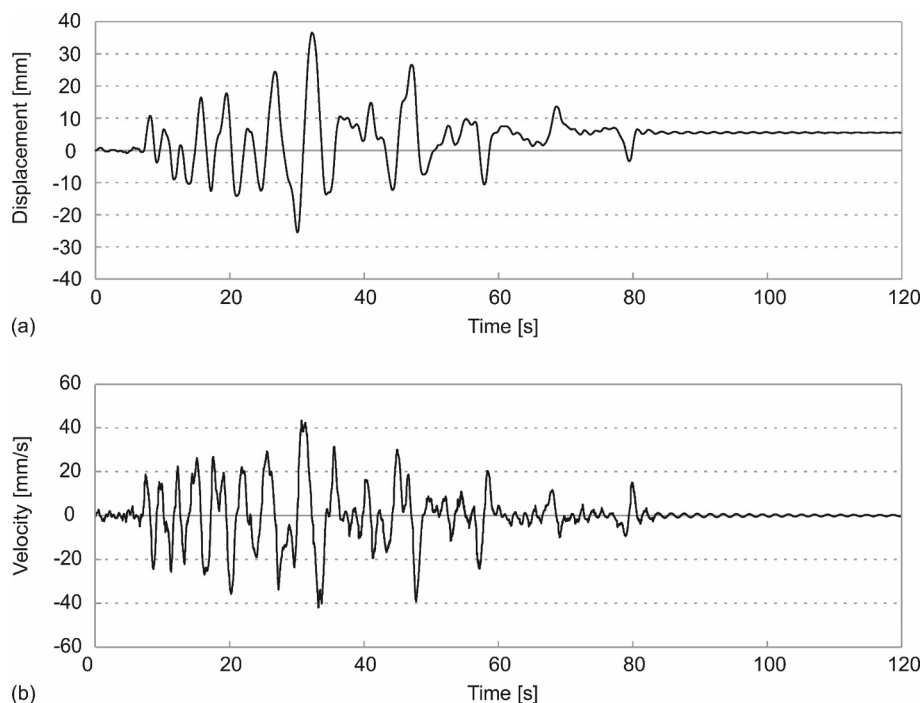
Fig. 7. Testing protocol for dynamic tests: (a) displacement response history and (b) velocity response history.
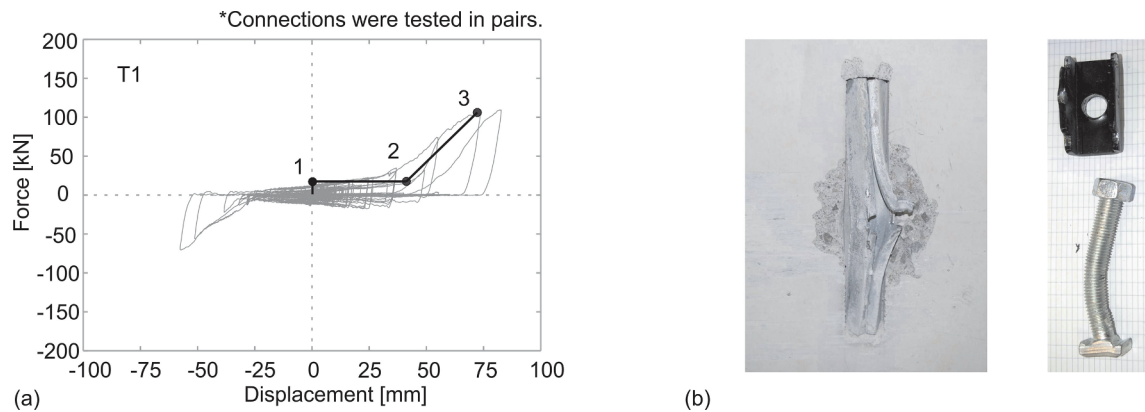
Fig. 8. Test of the top bolted connections: (a) typical hysteretic response of the top connections, (b) failed channel and deformed bolt.

is subjected to bending. Consequently, the lateral stiffness of the connection increases considerably (Fig. 8 between dots 2 and 3). Plastic deformations of the bolt and the channel cast in the column gradually increase.

(3) At the last stage, the failure of the connection is reached (dot 3 in Fig. 8). The connection typically fails due to the considerable plastic deformations of the channel and the bolt being pulled out (Figs. 8 and 9 Stage 3).

4.2. Response mechanism of the complete fastening system

The *response mechanism of the top connections,* observed within the experiments of the complete fastening systems was the same as described in the previous section.

The *response mechanism of the bottom cantilever connections* also consisted of three main stages, presented in Fig. 10:

(1) Initially, the friction force was activated (Fig. 10a) followed by the sliding of the panel. The friction was considerably smaller than in the top connections.

(2) When the available gap in the connection was exhausted (Fig. 10b), the stiffness of the connection increased considerably due to the bending of the cantilever bracket.

(3) Due to the large stiffness and the strength of the cantilever bracket, the response of the connection was predominantly elastic. At the end of the tests (which were mostly terminated since the total capacity of the hydraulic system was approaching) limited plastic deformations of the steel cantilever were observed (see Fig. 10c).

The response mechanisms of the top and bottom connections were, in general, similar. Thus, *the response mechanism of the complete fastening system* can also be characterized by three main stages (see the typical hysteretic response, presented in Fig. 11a):

(1) The friction force, which is activated in the top and bottom connections at the beginning of the tests, was approximately 20 kN. Mainly it was activated at the top connections (amounted to about 16 kN, see also Section 4.1 for more details).

(2) When the gaps in the top and the bottom connections were depleted at a displacement of around 4 cm (note that the gaps in the top and bottom connections were quite similar), the stiffness was considerably increased due to the activated bending stiffness of the bolts and the channels of the top connections and the bending stiffness of the cantilever brackets in the bottom connections. The comparison between the response of the complete fastening system and that of the top connections confirmed that the increase in the
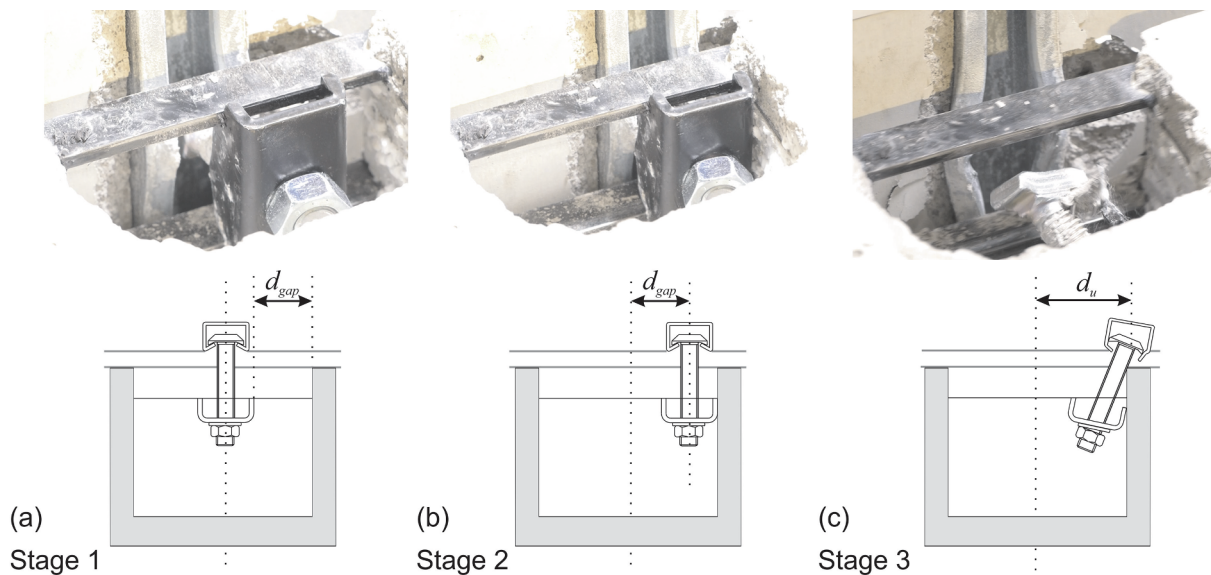
Fig. 9. Failure mechanism of the top bolted connections: (a) initial position, (b) the special bolt washer reaches the edge of the steel box profile cast in the panel, (c) failure due to the plastic deformations of the channel and the bolt being pulled out.
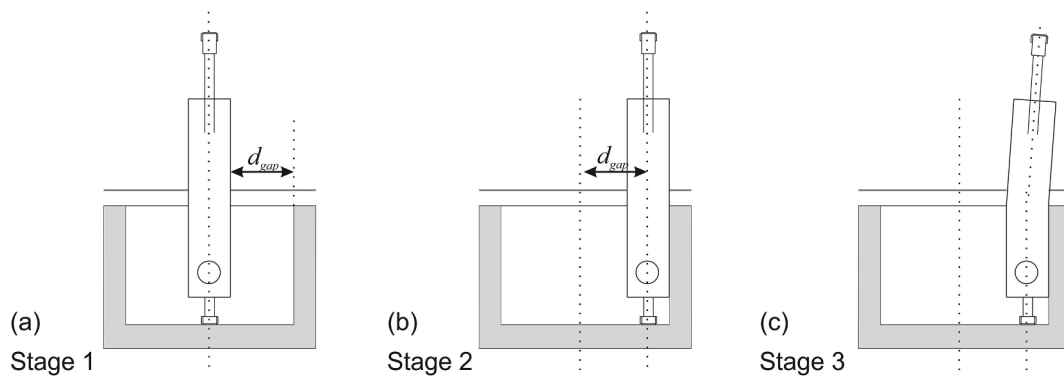
Fig. 10. The behaviour mechanism of the bottom bearing cantilever connection: (a) initial position, (b) the cantilever bracket reaches the edge of the opening and (c) minor deformations in the connection at the end of the test.

stiffness of the whole fastening system was considerably higher, mainly due to the activated bending stiffness of the cantilever bracket.

(3) Due to the depleted capacity of the actuator, the tests were terminated before the failure of the connections was achieved. At that moment, however, the top connections were considerably damaged, and the channels and bolts at the top were substantially and irreversibly deformed (see Fig. 11b). In some cases, also the concrete around the top connections was damaged (see Fig. 11c). The failure of the top connections was likely to occur at a relatively small increase in the displacement demand. Since at the same time, the damage to the bottom cantilever was minor (see Fig. 11b) it can be concluded that the failure of the whole fastening system would occur due to the failure of the top connection. This failure (as explained in Section 4.1) typically occurs due to the considerable plastic deformations of the channel and the bolt being pulled out.

In order to illustrate the previous observations, the response of the top connections and the whole fastening system are compared in Fig. 12. Both plots also show the corresponding envelope of the response (bold black line). In this particular case, the gaps at the top and the bottom connections were depleted approximately at the same time. Note, however, that this is not the rule and it depends on the construction tolerances (the bolt and the cantilever bracket may not be positioned centrally) as well as deformations of columns, which the panels are attached to.

In the presented tests, the panels were attached to a rigid beam. In real precast structures, the panels are fastened to deformable columns. Due to the columns' rotations and bending, the relative displacements between panels and columns (i.e. slips) at the level of top and bottom connections are different and can occur in the opposite directions. Note, however, that this does not affect basic response mechanisms or type of failure of the connection presented in the paper because the response of panels remains predominantly translational even when the columns are subjected to large rotations (bending).

The washer within the top connection is pinned by the bolt (see Fig. 3). Thus, it does not notably rotate despite the considerable rotations of columns. It can slide over the steel box profile in a similar manner as it was observed in the presented tests. Consequently, the panels do not rotate.

At the bottom connections, panels only lean on the steel stud. Thus, the rotations of the columns and the panels are different. It can be concluded that the bending of columns does not lead to rotations of panels, and the response of panels is predominantly translational.

Although columns rotations do not impose notable rotations of panels and connections, they cause different relative displacements between columns and panels at the level of top and bottom connections. At the strong seismic excitations, these displacements can occur in opposite directions. Nevertheless, this does not affect the basic response mechanisms or the hysteretic response of connections, observed within presented tests, because the response is independent of the direction of relative displacements.

In the presented tests, the top connections came first into contact with the panel at displacement $d_{gap,top}$. The stiffness of the fastening system was increased due to the increased stiffness of the top connections. When the displacement demand was increased to $d_{gap,bottom}$, the stiffness of the complete fastening system increased the second time (see Fig. 12b) due to the activated bending stiffness of the bottom connection. Both top and bottom connections were in contact with the panel.
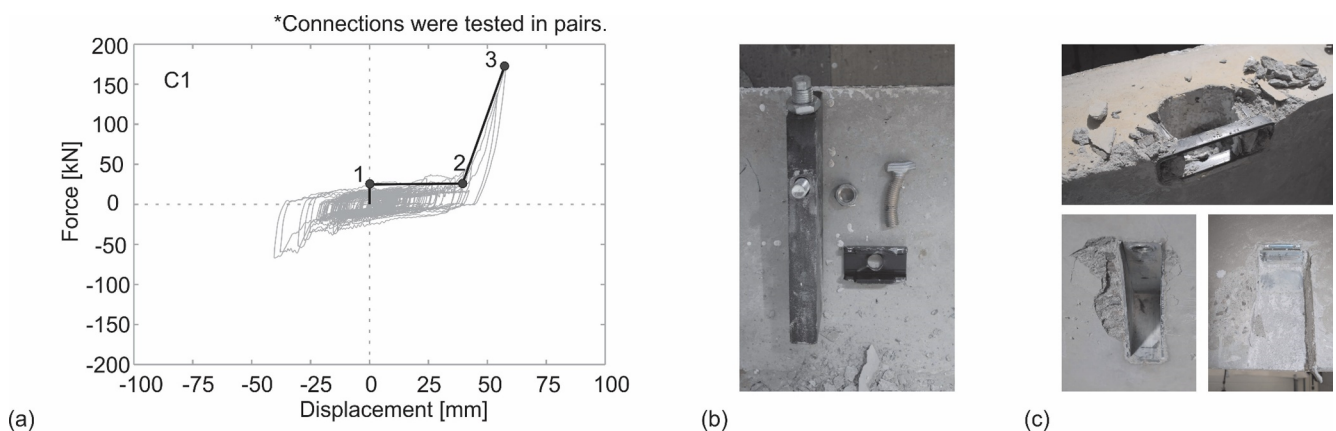
Fig. 11. Test of the complete fastening system: (a) typical hysteretic responses of the complete fastening system, (b) damaged connection parts after the test, and (c) damaged concrete around the connections after the test.
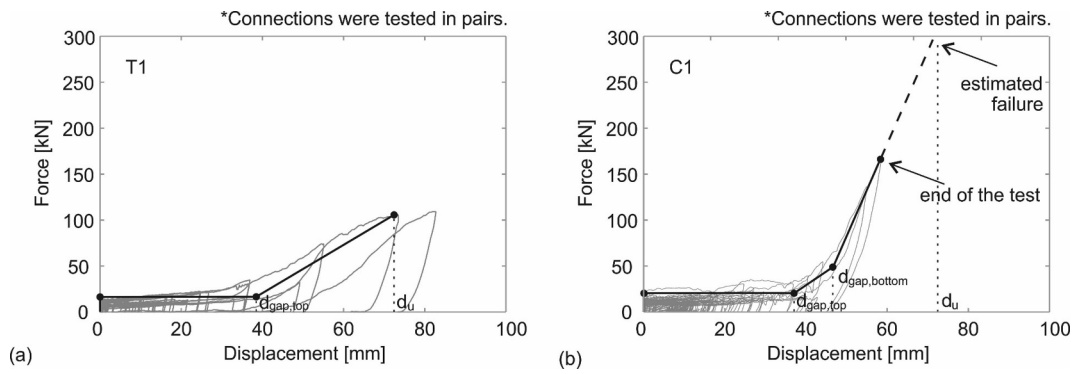
Fig. 12. Response envelopes of the connections: (a) top connections and (b) complete fastening system.

The test was terminated before the failure of the fastening system (due to the limitations of the actuator capacity). However, as explained and documented in the previous paragraphs, the top connections were subjected to considerable plastic deformations and were near collapse. Taking into account the displacement capacity of the top connections d_u observed in the tests (described in Section 4.1), and considering the almost elastic response of the bottom connections, the capacity of the fastening system was estimated as shown in Fig. 12 with a dashed line.

Because friction is low (see Fig. 12), it can be concluded that the panel can easily slide as long as the gaps are not depleted. If all the components of the fastening system are initially positioned at the centre, the gaps in both directions are the same, and the response will be symmetric. However, when a component is moved towards the edge, the response will be asymmetric. In such cases, the interaction between the panel and the columns in one direction could be activated at a smaller displacement demand.

It was observed that the friction in the fastening system was gradually reduced after several cycles, due to the bolt loosening at the top connections. This reduction was somewhat more pronounced after the contacts of the connections and the panel but did not have an important influence on the overall response. Due to the limitations of the actuator, only limited impact forces were observed.

5. Numerical modelling of the response

An attempt was made to formulate a macro numerical model,

capable of simulating the response of the top and bottom connections. It is presented in the following paragraphs. The model was built in the OpenSees framework [21] by combining different material models.

For the simulation of the bolted top connection response, three material models were combined: *ElasticPP (EPP)*, *ElasticPPGap (EPPGap)* and *Hysteretic*, as shown in Fig. 13a. The *ElasticPP* (Fig. 13b) model was used to simulate the friction between the steel elements (due to the tightening torque in the bolt). It was added in parallel to the series combination of the other two material models: the *ElasticPPGap* (Fig. 13c) and the *Hysteretic* (Fig. 13d), which are activated when the gap is depleted and the stiffness of the fastening system almost instantly increases.

The same numerical model (Fig. 13a) could also be used for modelling the response of the bottom connection. However, to be able to model the variable friction, observed during the dynamic tests, more accurately, the *EPP* model was replaced by the combined (in parallel) *Viscous* (Fig. 14b) and *Elastic* (Fig. 14c) material models. This model (Fig. 14a) takes into account that the friction force is dependent on the sliding speed and that the coefficient of friction between two objects varies according to the relative speed of motion [22,23].

In the literature, different friction models are available [24,25]. Commonly, the friction force is physically explained by the Coulomb friction behaviour as the product of normal force on the surface and the coefficient of friction that is generally acknowledged to be constant. In the presented tests (as well as in the real buildings, subjected to the seismic excitations) the panels were subjected to the dynamic load.
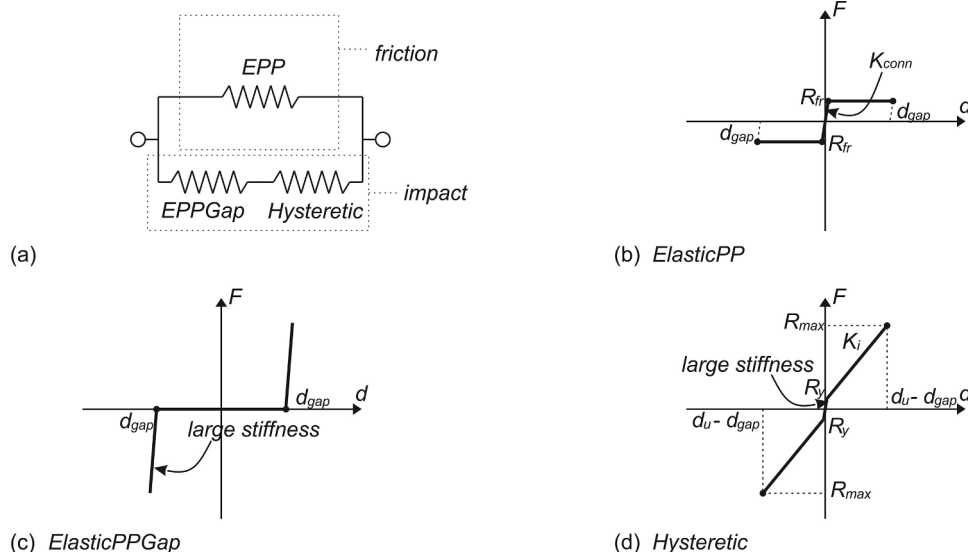
Fig. 13. Schematic presentation of the macro model: (a) combination of different hysteretic behaviours used for the numerical simulation of top and bottom connections, (b) ElasticPP, (c) ElasticPPGap and (d) Hysteretic behaviours.
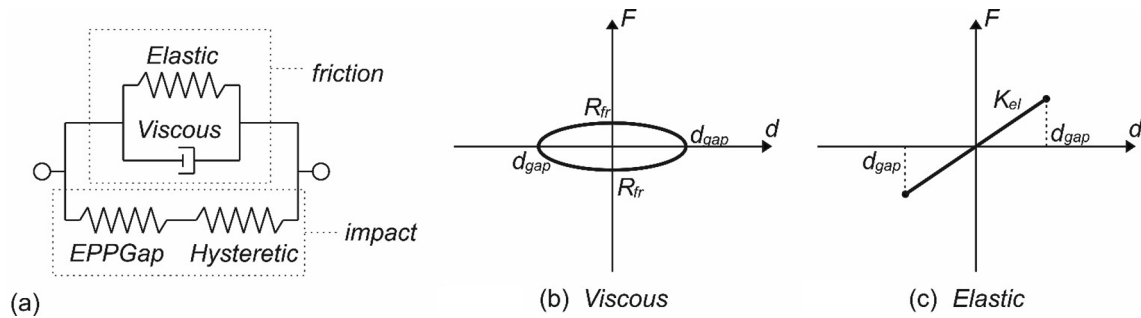
Fig. 14. Schematic presentation of the macro model: (a) a combination of different hysteretic behaviours used for the numerical simulation of the bottom connections under dynamic loading, (b) Viscous and (c) Elastic behaviours.
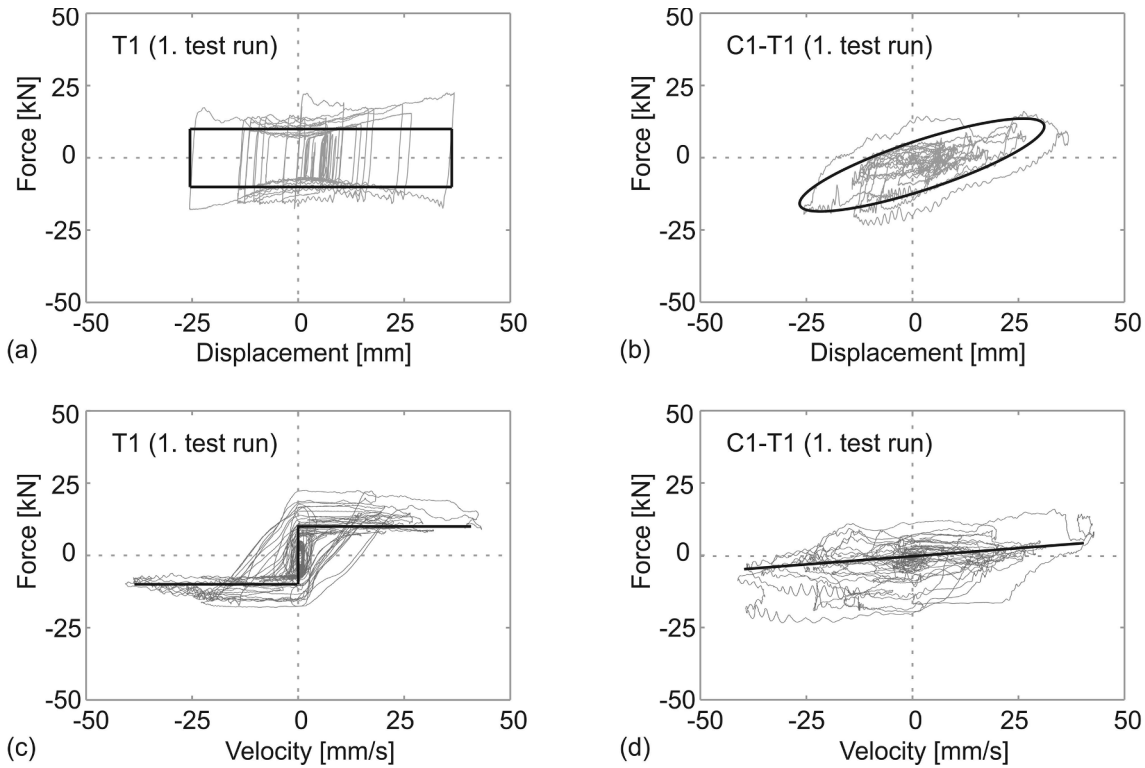
Fig. 15. Hysteretic responses (grey) and idealized envelopes (black): (a) force–displacement at top connection, (b) force–displacement at bottom connection (c) force–velocity at top connection (d) force–velocity at bottom connection.

Table 2
Recommended values of the parameters.

Material characteristic	Value	Material characteristic	Value
$c_{fr,top}$	0.4	$K_{conn,top}$	$2 \cdot 10^4$ kN/m
$d_{gap,top}$*	± 4.0 cm	$K_{i,top}$	$1.5 \cdot 10^3$ kN/m
$d_{gap,bottom}$*	± 4.5 cm	$K_{i,bottom}$	$3 \cdot 10^3$ kN/m
$c_{visc,bottom}$	50 t/s	$K_{el,bottom}$	200 kN/m
d_u*	± 7.5 cm	K_L	$1 \cdot 10^4$ kN/m
$px, py, d1, d2, b$	0, 0, 0, 0, 0	R_y	0.01 kN

Legend: $c_{fr,top}$ … friction coefficient between steel elements of the top connection, $d_{gap,top}$ … gap in the top connection, $d_{gap,bottom}$ … gap in the bottom connection, $c_{visc,bottom}$ … viscous damping coefficient, d_u … displacement capacity of the fastening system, $K_{conn,top}$ … initial stiffness of the top connection, $K_{i,top}$ …bending stiffness of the top connection, $K_{i,bottom}$ … bending stiffness of the bottom connection, $K_{el,bottom}$ …elastic stiffness of the bottom connection, K_L … large unloading stiffness after the gap is depleted, $px, py, d1, d2, b, R_y$ … specific parameters *pinchx, pinchy, damage1, damage2, beta* and R_y of the Hysteretic material model.

* Note that the value corresponds to the centrally positioned connections.

Thus, the friction force was considerably affected by the velocity of connections' excitations and damping, as already observed in [22,23]. The friction also depends on the surface treatment (e.g. cleanliness, lubrication) and the wear of the material during the movement. During the tests, the galvanised steel plates at the bottom connections have shown signs of substantial material wear.

For modelling the investigated fastening system, the Coulomb and viscous friction models were found to be the most appropriate, for the top and the bottom connections, respectively. The common Coulomb friction model assumes that the friction force is the product of the normal force on the surface and the constant coefficient of friction, whereas in the viscous friction model, the friction force is a linear function of the sliding speed.

In order to demonstrate that the Coulomb friction model is more appropriate for the top connections and the viscous friction model is more appropriate for the bottom cantilever connection, the typical response relationships (force–displacement and force–velocity) are shown for both connections in Fig. 15. A rough estimate of the response of the bottom connection was obtained by subtracting the response of the top connection from the response of the complete fastening system in two
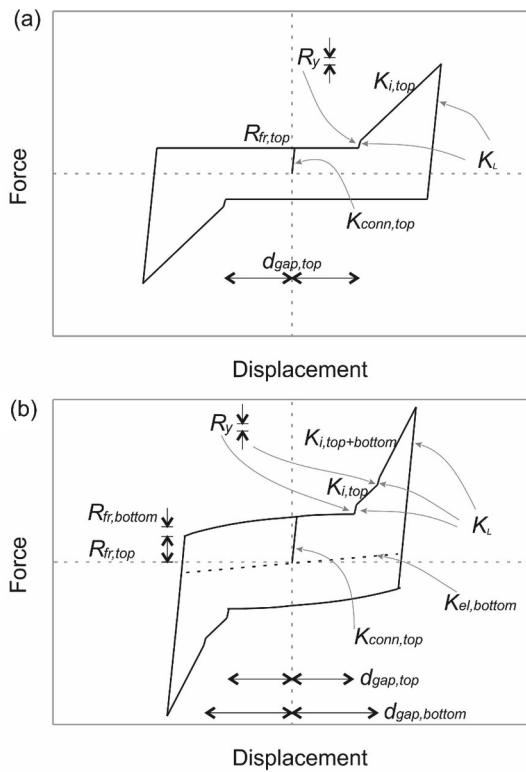
Fig. 16. Schematic envelopes of numerical models: (a) only the top connections and (b) the complete fastening system.

connections can be represented by the elastic-perfectly plastic response typical for Coulomb friction (Fig. 15a), whereas for the bottom connection viscous friction model is more appropriate (Fig. 15b). Similarly, the shape of force–velocity relationship ("S" shape) of the top connection is typical for Coulomb friction (Fig. 15c), whereas at the bottom connections this relationship has a shape, which is better represented by viscous friction model (Fig. 15d). In general, the response of the bottom connections is viscoelastic. Thus, for modelling the bottom connections, the viscous model combined with the elastic spring was used.

5.1. Model parameters

The results of the experiments were used to calibrate the numerical models. The following parameters were defined: the size of the gap (d_{gap}), the maximum displacement capacity (d_u), friction force (R_{fr}), damping (c_{visc}), and stiffness (K_{conn}, K_i, K_L) as explained in the following paragraphs. The recommended values are summarized in Table 2. The efficiency of the proposed numerical models is demonstrated in Figs. 16-18. The force–displacement relationships (i.e. envelopes) of the numerical models used are schematically presented in Fig. 16, whereas in Fig. 17, the experimental and numerical hysteretic responses are compared.

With the proposed macro models, a satisfying match between the experimental and numerical results was achieved. To better evaluate the calibration, graphs of the accumulated hysteretic energy are shown in Fig. 18.

5.2. Size of the gap

In the tests, the size of the gap of the top and the bottom connection was approximately the same - about 4 cm. This is half of the available space in the panel (see Figs. 3 and 4) reduced by half of the thickness of the bolt and the cantilever bracket.

initial test runs with identical loading protocols and the same tightening torque.

The force–displacement relationship typically observed in top
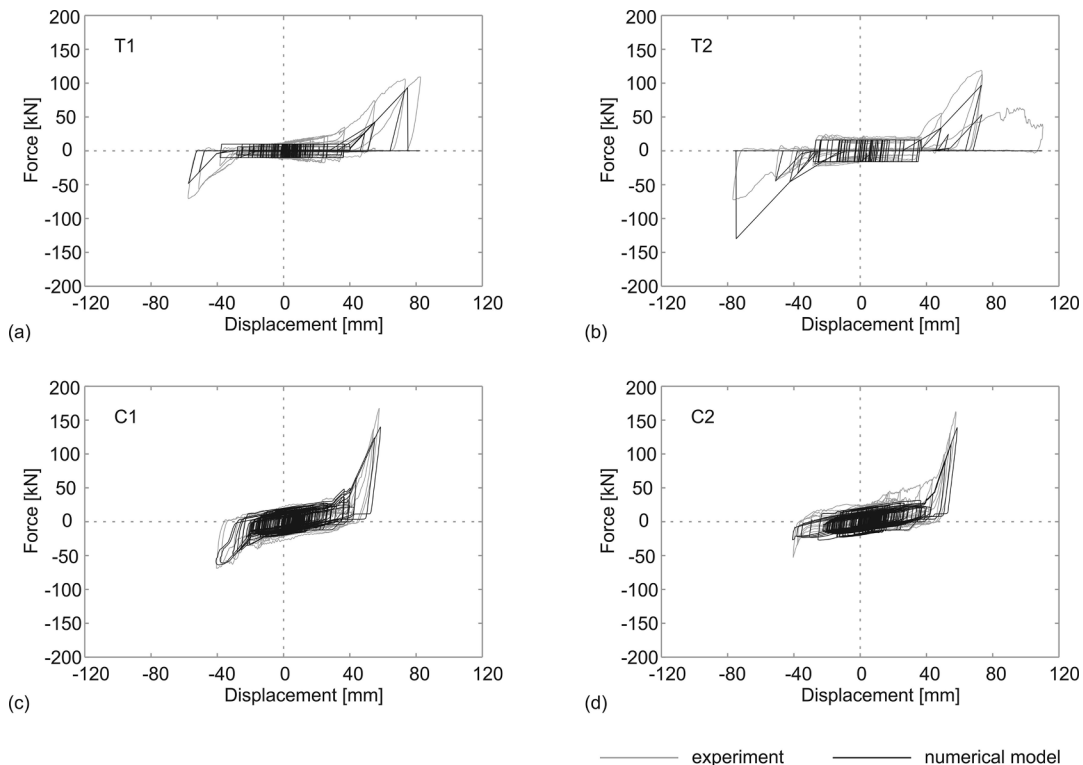
Fig. 17. A comparison of the experimental (grey) and the numerical (black) hysteretic responses: (a) and (b) only the top connections, (c) and (d) the complete fastening system.
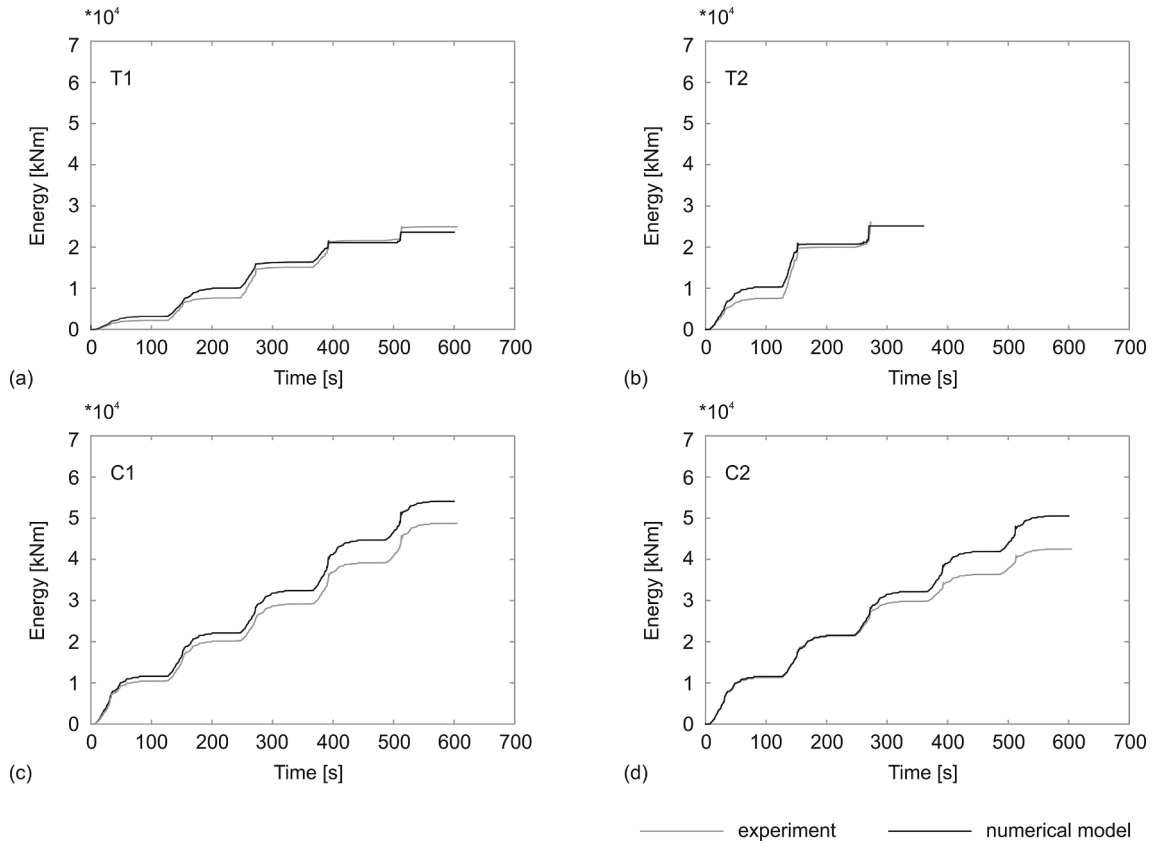
Fig. 18. A comparison of the accumulated hysteretic energy during the experiments (grey) and the numerical simulation (black): (a) and (b) only the top connections, (c) and (d) the complete fastening system.

Note, however, that the size of the gap is importantly influenced by the construction tolerances. In the tests, the bolt and the cantilever bracket were positioned approximately in the centre. During the construction in real buildings, this position can be very eccentric. Since this can importantly influence the interaction between the panel and the column, it is proposed to consider central and extreme positions in analyses.

5.3. Displacement capacity

According to the tests, the displacement capacity of the top connection was between 7 and 8 cm (relative displacements between the panel and the main structure). This can be considered as the displacement capacity of the complete connection assembly since the top connections are the weakest component (please see the discussion about the failure, provided in Section 4.2).

The displacement capacity addressed above corresponds to the gap size of 4 cm. If the gap size is smaller because of the eccentrically positioned panel, the displacement capacity will be reduced to:

$$d_u = min d_{gap,top} + 4 \; cm \tag{1}$$

5.4. Friction

The friction activated in the connection influences the level of the interaction between the panel and the columns of the main building. The greater the friction force, the stronger the interaction between the panel and the columns is provided.

During the experiments, the maximum friction force of $R_{fr,top} = 8$ kN was observed at the top connections (note that the connections were tested in pairs). This force can be estimated based on the friction coefficient $c_{fr,top}$ and the tightening force in the bolt F_b:

$$R_{fr} = c_{fr,top} F_b \tag{2}$$

$$F_b = \frac{T_b}{c_0 D_b} \tag{3}$$

where T_b is the tightening torque in the bolt, c_0 is the friction coefficient in the threaded bolt, which is equal to 0.2 [26], and D_b is the nominal diameter of the bolt. For the investigated connections, the friction coefficient $c_{fr,top} = 0.4$ is recommended. It was obtained based on the ratio between the measured friction forces ($R_{fr,top} = 8$ kN) and the tightening force ($F_b = 20$ kN, corresponding to the tightening torque $T_b = 65$ Nm). The proposed value is in quite good agreement with the friction coefficients evaluated by Del Monte et al. [7].

The typical friction force at the bottom connection $R_{fr,bottom}$ was estimated subtracting the friction force of the top connections from that observed during the tests of the complete fastening system. The total friction force of the complete fastening system was 20 kN. The frictional resistance of the two top connections was 16 kN. Thus, the friction in the bottom connections was 4 kN in total or 2 kN per one connection. It was four times smaller than that at the top connections. Note, however, that the friction in the top connection strongly depends on the tightening torque in the bolt. When the torque is small, the friction of the top connection will also be reduced to about 2 kN.

5.5. Damping

The recommended value of the damping coefficient $c_{visc,bottom}$ for the *Viscous* model was estimated based on the velocity and friction force measured in the tests. Later on, the coefficient was calibrated with numerical simulations, and the final value of 50 t/s was defined. It corresponds to a force of 2 kN at a velocity of 0.04 m/s.

5.6. Stiffness

In general, the initial stiffness of the top connections ($K_{conn,top}$) is very large as long as the full friction force is not activated (see the recommended values in Table 2). After that, stiffness is almost 0 until the gap is depleted. Then it abruptly increases to K_i due to the bending stiffness of the top bolt. The experimentally estimated values are similar to those proposed by Belleri et al. [5].

The *Hysteretic* material model was used to model the response after the gap was closed. All the following specific parameters should be set to 0 for this purpose: *pinchx*, *pinchy*, *damage1*, *damage2* and *beta*. The parameter R_y of the *Hysteretic* model behaviour (see the envelopes in Fig. 18) should be small since it is intended only to define the large unloading stiffness K_L after the gap has been depleted.

6. Conclusions

The paper presents the experimental and analytical studies of the fastening system which is typically used in Central Europe to attach horizontal cladding panels to the columns of RC precast buildings. The system consists of two main parts: (1) the pair of top bolted connections, which provide stability to the panel, subjected to the horizontal excitations, and (2) the pair of bottom cantilever connections, which support the weight of the panel.

A typical response mechanism of the complete fastening system consists of three distinct stages: sliding with limited friction, contact with the panel causing the increase in the connection stiffness, and the failure. It was found that the failure of the fastening system in an earthquake occurs when the in-plane displacement capacity of the bolted top connection is depleted. At this point, the stability of the entire panel is compromised.

The capacity of the fastening system should be expressed in terms of displacements, rather than in terms of strength because the capacity of the system is limited by the displacement capacity of the top connection. The displacement capacity depends on the construction tolerances and the initial size of the gaps. The deformation capacity is about 4 cm larger than the initial gap size of the top connection.

The initial gap size depends on the construction. Since it may influence the response and since it is not known in advance, it is recommended to take into account two extreme cases: centrally mounted connections (the gap size in both directions is the same), and eccentrically positioned bolts and cantilever brackets.

Experimental force–displacement responses of the tested connections were used to propose a new numerical model, which is able to describe the in-plane behaviour of the tested fastening system under dynamic loading. The new numerical model is formulated by combining different material models available in the OpenSees framework. The typical values of different parameters needed to define the model are proposed and calibrated by the experiments.

The analysis confirmed that the responses of the top and bottom connections have somewhat different characteristics. The top connection appears to exhibit typical Coulomb friction behaviour, whereas the viscoelastic behaviour better describes the response of the bottom connection. The numerical model was validated by dynamic tests and a satisfying match between the experimental and numerical results was achieved.

Declaration of Competing Interest

None.

Acknowledgements

References

[1] Bournas DA, Negro P, Taucer FF. Performance of industrial buildings during the Emilia earthquakes in Northern Italy and recommendations for their strengthening. Bull Earthq Eng 2013;12:2383–404. https://doi.org/10.1007/s10518-013-9466-z.

[2] Magliulo G, Ercolino M, Petrone C, Coppola O, Manfredi G. The Emilia earthquake: Seismic performance of precast reinforced concrete buildings. Earthq Spectra 2014;30:891–912. https://doi.org/10.1193/091012EQS285M.

[3] Savoia M, Buratti N, Vincenzi L. Damage and collapses in industrial precast buildings after the 2012 Emilia earthquake. Eng Struct 2017;137:162–80. https://doi.org/10.1016/j.engstruct.2017.01.059.

[4] SAFECLADDING. SAFECLADDING project – Improved Fastening Systems of Cladding Wall Panels of Precast Buildings in Seismic Zones. http://www.safe-cladding.eu. 2015.

[5] Belleri A, Torquati M, Marini A, Riva P. Horizontal cladding panels: in-plane seismic performance in precast concrete buildings. Bull Earthq Eng 2016;14:1103–29. https://doi.org/10.1007/s10518-015-9861-8.

[6] Belleri A, Cornali F, Passoni C, Marini A, Riva P. Evaluation of out-of-plane seismic performance of column-to-column precast concrete cladding panels in one-storey industrial buildings. Earthq Eng Struct Dyn 2018;47:397–417. https://doi.org/10.1002/eqe.2956.

[7] Del Monte E, Falsini C, Boschi S, Menichini G, Orlando M. An innovative cladding panel connection for RC precast buildings. Bull Earthq Eng 2019;17:845–65. https://doi.org/10.1007/s10518-018-0470-1.

[8] CEN. Eurocode 8: Design of structures for earthquake resistance - Part 1: General rules, seismic actions and rules for buildings. Brussels: European Committee for Standardisation; 2004.

[9] Toniolo G, Colombo A. Precast concrete structures: the lessons learned from the L'Aquila earthquake. Struct Concr 2012;13:73–83. https://doi.org/10.1002/suco.201100052.

[10] Fischinger M, Zoubek B, Isaković T. Seismic response of precast industrial buildings. In: Ansal A, editor. Perspect. Eur. Earthq. Eng. Seismol. Volume 1, Berlin: Springer; 2014, p. 131–77.

[11] Negro P, Lamperti Tornaghi M. Seismic response of precast structures with vertical cladding panels: The SAFECLADDING experimental campaign. Eng Struct 2017;132:205–28. https://doi.org/10.1016/j.engstruct.2016.11.020.

[12] Toniolo G, Dal Lago B. Conceptual design and full-scale experimentation of cladding panel connection systems of precast buildings. Earthq Eng Struct Dyn 2017;46:2565–86. https://doi.org/10.1002/eqe.2918.

[13] Psycharis IN, Kalyviotis IM, Mouzakis HP. Experimental investigation of the response of precast concrete cladding panels with integrated connections under monotonic and cyclic loading. Eng Struct 2018;159:75–88. https://doi.org/10.1016/j.engstruct.2017.12.036.

[14] Yüksel E, Karadoğan F, Özkaynak H, Khajehdehi A, Güllü A, Smyrou E, et al. Behaviour of steel cushions subjected to combined actions. Bull Earthq Eng 2018;16:707–29. https://doi.org/10.1007/s10518-017-0217-4.

[15] Zoubek B, Fischinger M, Isaković T. Cyclic response of hammer-head strap cladding-to-structure connections used in RC precast building. Eng Struct 2016;119:135–48. https://doi.org/10.1016/j.engstruct.2016.04.002.

[16] Colombo A, Negro P, Toniolo G, Lamperti M. Design Guidelines for Precast Structures with Cladding Panels. 2016. https://doi.org/10.2788/956612.

[17] Colombo A, Lamperti M, Negro P, Toniolo G. Design Guidelines for Wall Panel Connections. 2016. https://doi.org/10.2788/546845.

[18] Scotta R, De Stefani L, Vitaliani R. Passive control of precast building response using cladding panels as dissipative shear walls. Bull Earthq Eng 2015;13:3527–52. https://doi.org/10.1007/s10518-015-9763-9.

[19] Zoubek B, Isaković T, Janković G, Fischinger M. Intermediate report 1.1: Dynamic tests on cladding-to-structure connections. Ljubljana 2016.

[20] ZAG. Equipment overview 2019. http://www.zag.si/en/equipment.

[21] McKenna F, Fenves GL. Open System for Earthquake Engineering Simulation (OpenSees); 2010. http://opensees.berkeley.edu.

[22] Kragelskii IV. Friction and Wear. London: Butterworths; 1965.

[23] Rabinowicz E. Stick and Slip. Sci Am 1956;194:109–18.

[24] Andersson S, Söderberg A, Björklund S. Friction models for sliding dry, boundary and mixed lubricated contacts. Tribol Int 2007;40:580–7. https://doi.org/10.1016/j.triboint.2005.11.014.

[25] Liu YF, Li J, Zhang ZM, Hu XH, Zhang WJ. Experimental comparison of five friction models on the same test-bed of the micro stick-slip motion system. Mech Sci 2015;6:15–28. https://doi.org/10.5194/ms-6-15-2015.

[26] Zoubek B. Influence of the connections on the seismic response of precast reinforced concrete structures. University of Ljubljana 2015.